

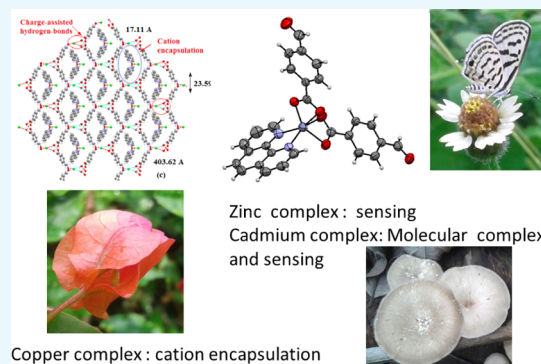
Copper(II), Zinc(II), and Cadmium(II) Formylbenzoate Complexes: Reactivity and Emission Properties

Jitendra Nath, Arup Tarai, and Jubaraj B. Baruah*[✉]

Department of Chemistry, Indian Institute of Technology Guwahati, Guwahati 781 039, Assam, India

Supporting Information

ABSTRACT: Synthesis, characterization, reactivity, and sensing properties of 4-formylbenzoate complexes of copper(II), zinc(II), and cadmium(II) possessing the 1,10-phenanthroline ancillary ligand are studied. The crystal structures of the (1,10-phenanthroline)bis(4-formylbenzoate)(aqua)copper(II) and (1,10-phenanthroline)bis(4-formylbenzoate)zinc(II) and a novel molecular complex comprising an assembly of mononuclear and dinuclear species of (1,10-phenanthroline)bis(4-formylbenzoate)cadmium(II) are reported. These zinc and cadmium complexes are fluorescent; they show differentiable sensitivity to detect three positional isomers of nitroaniline. The mechanism of sensing of nitroanilines by 1,10-phenanthroline and the complexes are studied by fluorescence titrations, photoluminescence decay, and dynamic light scattering. A plausible mechanism showing that 1,10-phenanthroline ligand-based emission quenched by electron transfer from the excited state of 1,10-phenanthroline to nitroaniline is supported by density functional theory calculations. In an anticipation to generate a fluorescent d^{10} -copper(I) formylbenzoate complex by a mild reducing agent such as hydroxylamine hydrochloride for similar sensing of nitroaromatics as that of the d^{10} -zinc and cadmium 4-formylbenzoate complexes, reactivity of d^9 -copper(II) with hydroxylamine hydrochloride in the presence of 4-formylbenzoic acid and 1,10-phenanthroline is studied. It did not provide the expected copper(I) complex but resulted in stoichiometry-dependent reactions of 4-formylbenzoic acid with hydroxylamine hydrochloride in the presence of copper(II) acetate and 1,10-phenanthroline. Depending on the stoichiometry of reactants, an inclusion complex of bis(1,10-phenanthroline)(chloro)copper(II) chloride with in situ-formed 4-((hydroxyimino)methyl)benzoic acid or copper(II) 4-(hydroxycarbonyl)benzoate complex was formed. The self-assembly of the inclusion complex has the bis(1,10-phenanthroline)(chloro)copper(II) cation encapsulated in hydrogen-bonded chloride-hydrate assembly with 4-((hydroxyimino)methyl)benzoic acid.



INTRODUCTION

Self-assemblies of metal complexes are prospective candidates for optical devices.^{1–5} The photoluminescence of small inorganic complexes is an emerging topic of research in the detection of pollutant and hazardous materials.^{6–19} Functional modifications on coordinated ligands are used in various inorganic syntheses.^{20–24} Such reactions are extended to prepare coordination polymers,²⁵ poly-nuclear complexes,^{26–28} rotaxanes, and catenanes.^{29–31} Hydrolytic transformations of functional groups are in use to prepare coordination polymers,³² to modify metallo–organic frameworks³³ and dendrimers.^{34,35} The transformations of functional groups of framework structures, polymers, and nano-dimensional materials are of general interest to chemical sciences.^{36–39} The functional groups of fluorescent compounds influence detection ability of certain analytes.⁴⁰ Some functional groups of metallo–organic frameworks are responsible for sensing volatile organic compounds. For example, aldehyde-containing metallo–organic frameworks are used to detect amines.^{41,42} The weak interactions of photoluminescent analytes^{6–19} are useful to divulge emission paths. For instance, mechano-

responsive self-assemblies of luminescent frameworks are designed by enhancing π – π , C–H $\cdots\pi$ interactions.⁴³ Alternatively, the noncovalent interactions of functional groups of a metal complex are utilized to construct second-coordination sphere of metal complexes.^{44,45} Photoluminescence properties of a compound depend on π -stacking arrangements; face to face, edge to face π -stacks show different photoluminescences.^{46,47} Furthermore, the π -interactions of metallo–organic frameworks are modulated to show white-light emission.⁴⁸ The π -interactions of ligands are also useful in molecular recognition.⁴⁹

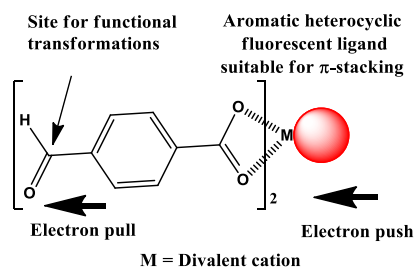
The low-nuclear complexes are the primary building constituents of many multinuclear complexes and noncovalent assemblies. Hence, diverse ways of weak interactions of small inorganic building blocks affecting photoluminescence properties are imperative. We choose here to study the sensing and the reactivity of mononuclear species shown in Scheme 1. This

Received: August 28, 2019

Accepted: October 17, 2019

Published: October 25, 2019

Scheme 1. Representation of Electronic Push–Pull Effect in a Portion of a Metal Complex Possessing Fluorescent Ligand Suitable for π -stacking



represents a mononuclear species suitable to form poly-nuclear complexes and has option for chemical and optical sensing of different substrates. Chemosensing by such a species would occur through several ways; out of them, three prominent ways are (i) improvisations of electronic effects of the metal ion, including possible redox-reaction causing chemical transformations; (ii) transformation of the aldehyde functional group of the 4-formylbenzoate to another functional group; (iii) utilization of the weak interactions to form self-assemblies. The species shown in Scheme 1 has also the qualities to form aggregates for aggregation-induced emission, or for intramolecular charge transfer, or exciplex to affect the fluorescence emission from itself or on another interacting species. Each of these is important to study the sensing ability of an analyte. The 4-formylbenzoate on the species is electron-withdrawing to extend its electronic effect to another fluorescent ligand of the complex through the intervening metal ion. The electronic effects of diamagnetic metal complexes possessing electron-rich and -deficient ligands cause signal transduction through intramolecular charge transfer.^{50,51} Push–pull electronic effects of zinc complexes of multipolar ligands cause extensive solvato-emissive effects.^{4,5} Wide applications of metallo–organic frameworks as optical materials and sensors make one curious to study discrete units of a framework to understand properties.^{52,53} There are also many self-assembled aggregates comprising multiple neutral species of zinc,^{54,55} manganese,⁵⁶ copper carboxylates.^{57,58} Depending on the electronic configuration of the central metal-ion, the inherent magnetic properties of the metal ion directly influence the photoluminescence OFF or ON states. A diamagnetic 4-formylbenzoate complex with 1,10-phenanthroline-based ligand would assist in intramolecular charge transfer, whereas a paramagnetic metal complex will be in general nonemissive. However, a nonemissive compound may be suitable for signal transductions through chemosensing upon concealing the metal ion or functionalization of the aldehyde functional group or other associative and dissociative processes. Hence, there are scopes to study chemosensing of those paramagnetic complexes of naturally abundant copper(II) ions by reacting with a mild reducing agent such as hydroxylamine. To understand the electronic effects and reactivity associated with the mononuclear model complexes of d^9 -copper, d^{10} -zinc, and d^{10} -cadmium possessing the features discussed above, sensing properties of 1,10-phenanthroline-containing complexes of copper(II), zinc(II), and cadmium(II) 4-formylbenzoate complexes are presented in this article (Figure 1).

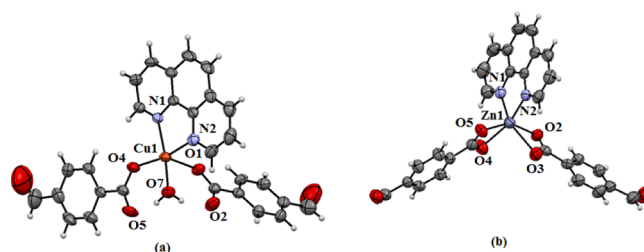


Figure 1. Structure of complexes (a) **1** and (b) **2** (drawn with 50% thermal ellipsoids). The metal to ligand bond distances (in Å) in the copper complex are Cu1–O1, 1.945 (4); Cu1–O7, 1.986 (4); Cu1–N2, 2.017 (4); Cu1–N1, 2.023 (4); Cu1–O4, 2.300 (4), whereas in the zinc complex they are Zn1–O5, 2.005 (2); Zn1–O2, 2.090 (2); Zn1–N2, 2.097 (2); Zn1–N1, 2.109 (3); Zn1–O3, 2.179 (2); Zn1–O4, 2.410 (2).

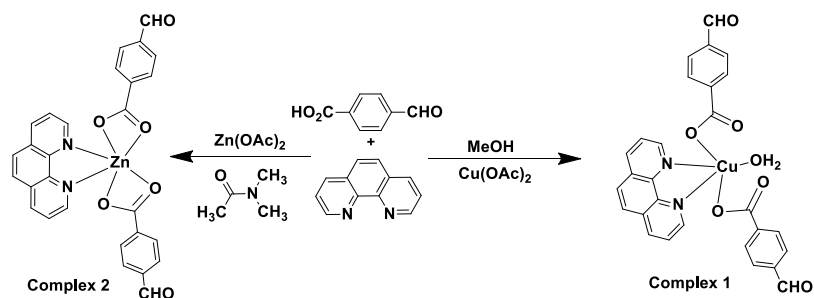
RESULTS AND DISCUSSION

Synthesis and Characterization of Zinc and Copper Formylbenzoate Complexes.

The mononuclear complexes **1** and **2** shown in Scheme 2 are obtained from the reactions of 4-formylbenzoic acid with zinc(II) acetate or copper(II) acetate in the presence of 1,10-phenanthroline. The copper complex **1** is a six-coordinate; it has two monodentate carboxylates, one bidentate 1,10-phenanthroline along with a water molecule coordinating to the copper(II) ion. The complex adopts a distorted square-pyramidal geometry, in which one of the 4-formylbenzoate occupies the axial position and the rest of the ligands constitute the base of the square (Figure 1a). The planar base comprises an O-atom of water, an oxygen of formylbenzoate, two nitrogen atoms of 1,10-phenanthroline each coordinating to a copper(II) ion. The Cu1–O2 and Cu1–O5 distances are 3.267, 3.302 Å, respectively, which indicate that the O2 and O5 atoms are not sufficiently close to form a copper oxygen bond. The bond distances of the two Cu–O bonds of the monodentate carboxylates, namely, Cu1–O1, 1.945 (4) Å and Cu–O4, 2.300 (4) Å are dissimilar. The axial bond of the square pyramid is a relatively longer Cu1–O4 bond than the other bonds because of the Jahn–Teller effect. The Cu1–O7 distance is 1.986(4) Å, and shows a strong binding of the water molecule to the copper ion. The coordinated water molecule is involved in intramolecular hydrogen bonds with the C=O bonds of the carboxylate groups. The IR spectra of the complex have C=O stretching for the aldehyde group at 1692 cm^{-1} and O–H stretching of water molecules at 3439 cm^{-1} . The carboxylate C=O stretching appears at 1595 cm^{-1} . The electron spin resonance (ESR) spectra of the complex have a broad signal at $g = 2.103$ at room temperature; it shows copper is at the +2 oxidation state in the complex. Complex **1** is formed as the sole product in the reaction, as the recrystallized bulk material shows an identical powder X-ray diffraction (XRD) pattern as that of the theoretically generated powder XRD pattern from the crystallographic information file of complex **1**.

The zinc complex **2** is a six-coordinate complex having two bidentate carboxylates and bicoordinating 1,10-phenanthroline (Figure 1b). The Zn–O bond distances are in the range of 2.005–2.410 Å and the two Zn–N bonds are 2.097(2) and 2.109(3) Å, respectively, establishing their bicoordination modes to the zinc ion. The 1,10-phenanthroline-containing zinc carboxylate complexes may form mononuclear or dinuclear complexes depending on carboxylic acids.⁵⁹ The

Scheme 2. Synthesis of Copper and Zinc 4-Formylbenzoate complexes



Scheme 3. Reaction of 4-Formylbenzoic Acid with Hydroxylamine Mediated by Copper(II) Acetate

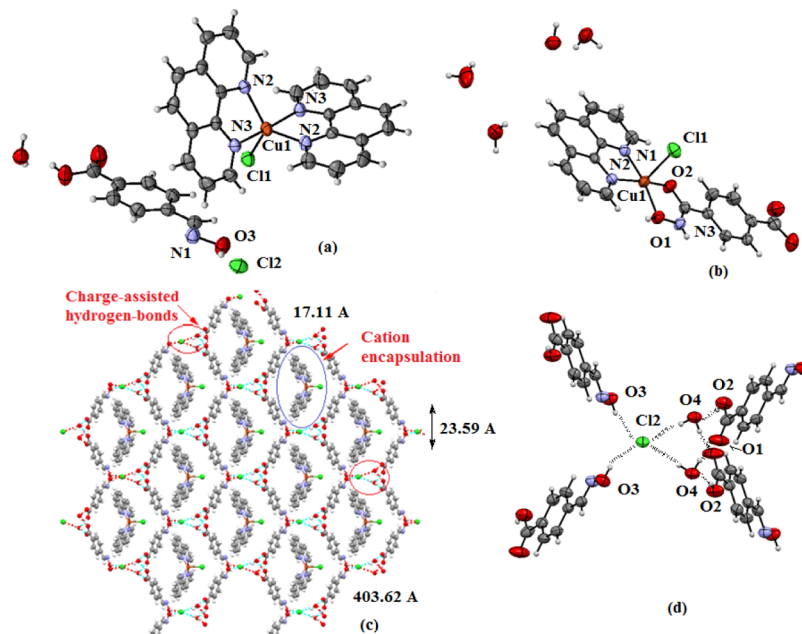
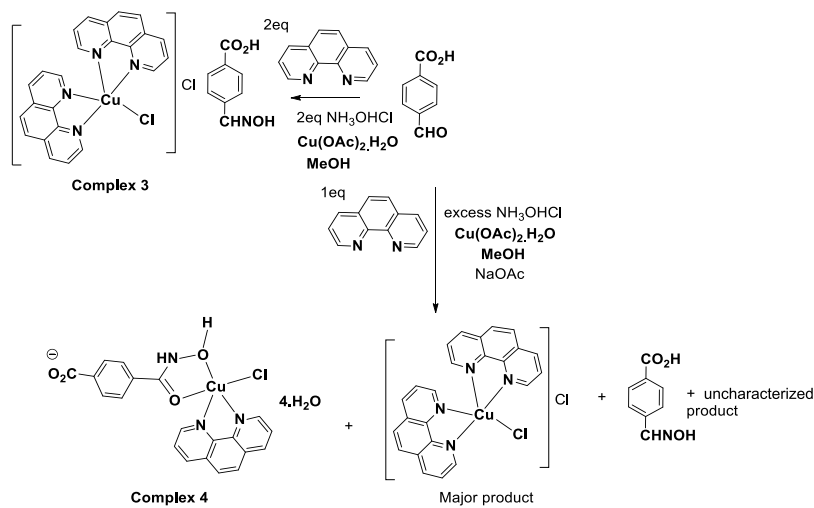


Figure 2. X-ray crystal structure of (a) complex 3, (b) complex 4, (c) self-assembly of complex 3, and (d) is the portion of the assembly of 3 showing hydrogen bonds to provide the junction to form enclosures for cation encapsulation.

observed zinc–oxygen bonds of the formylbenzoate tally with the reported carboxylates chelating zinc ions. In solution, the complex has ¹H NMR signals for aldehyde C–H at 10.01 ppm. The two sets of hydrogen atoms of the 4-formylbenzoate appear in the AA'BB' pattern. They appear as doublet of

doublet centering at 7.86 and 8.03 ppm, whereas there are signals from the three magnetically nonequivalent sets of hydrogen atoms of 1,10-phenanthroline at 8.25, 8.86, 9.21 ppm, respectively. The bischelation of 4-formylbenzoate is reflected in the carbonyl stretching of carboxylate observed at

1643 cm^{-1} . The aldehyde carbonyl $\text{C}=\text{O}$ stretching appears at 1702 cm^{-1} . The powder XRD of the bulk sample of the complex tallies with the one obtained from the crystallographic information file, which shows not only bulk purity of the sample but also confirms the single product obtained from the reaction.

Reactivity of 4-Formylbenzoic Acid toward Hydroxylamine in the Presence of Copper(II) Ions. When copper(II) acetate, 1,10-phenanthroline, and 4-formylbenzoic acid were reacted in 1:2:2 mole ratios followed by a reaction with 2 moles of hydroxylamine hydrochloride, an inclusion complex **3** was formed (Scheme 3). The complex has IR stretching at 3395 cm^{-1} because of the O–H group and at 1688 cm^{-1} because of the free carboxylate group. At room temperature, the complex shows a broad ESR signal at $g = 2.095$; which is characteristic of a d^9 electronic configuration, suggesting it to be a copper(II) complex. The cationic part of the complex comprises of a copper(II) ion coordinated to two bidentate 1,10-phenanthroline ligands and a chloride ligand. It has a distorted square pyramidal geometry. The charge of the complex cation is neutralized by a chloride ion located outside the coordination sphere (Figure 2a). The cationic part has an umbrella-like shape, where the cover of the umbrella-like shape comprises the copper ion coordinating to two 1,10-phenanthroline ligands and the rod of the umbrella-like shape is the copper–chloride bond. The symmetric nature of the cation with respect to mirror planes is reflected in the similar Cu1–N2 and Cu1–N3 bond distances of the two independent 1,10-phenanthroline ligands. The bond distances are Cu1–N2, 2.009 (3) Å and Cu1–N3, 2.095(2) Å, respectively. The Cu1–Cl1 bond distance is 2.298 (4) Å. The anionic portion of the self-assembly of the complex is an example of the utilization of three different aspects of supramolecular chemistry, namely (a) halide–water interactions,^{60–65} (b) charge-assisted hydrogen bonds,⁶⁶ and (c) anion coordination.^{67,68} Complex **3** forms a charge-assisted hydrogen-bonded 2D network possessing a grid-like structure encapsulating the complex cations. Each chloride ion in the self-assembly has a four-coordinate hydrogen-bonded environment. It is connected to two oxime molecules (Figure 2d) through O3–H...Cl2 hydrogen-bonds [$d_{\text{D}\cdots\text{A}} = 3.128(3)$ Å, $\angle\text{D}\cdots\text{H}\cdots\text{A}$, 154°]. However, the two water molecules are linked to the chloride ion through two charge-assisted hydrogen bonds O4–H...Cl2 hydrogen bonds [$d_{\text{D}\cdots\text{A}} = 3.228(3)$ Å, $\angle\text{D}\cdots\text{H}\cdots\text{A}$, 166(4)°]. The water molecules coordinating to the chloride ion also act as bridges by forming hydrogen bonds (bond parameters listed in Table S1) with the carboxylic acid groups of two independent molecules of oxime of the 4-formylbenzoic acid. The complex cations having an umbrella-like shape are located at these voids of about 403 Å² area (Figure 2c). Oximes are well-known to form molecular complexes.^{69,70} *t*-Butylammonium cation encapsulations by hydrogen bonded assemblies of halide with oxime were reported earlier by us.⁷¹ Some oximes also get encapsulated in coordination polymers.^{72,73} In the present case, the self-assembly of complex **3** has hydrated chloride ions that are hydrogen bonded to oximes providing spaces to encapsulate pentacoordinated copper(II) complex cations.

Excess amounts of hydroxylamine hydrochloride reacted with a mixture of copper(II) acetate, 4-formylbenzoic acid, and 1,10-phenanthroline in a mole ratio of 1:1:1, providing a new complex **4** (Figure 2b). The complex has 4-(hydroxycarbamoyl)benzoate (Scheme 3) as one of the

ligands. The complex has IR stretching at 3403, 1721, and 1679 cm^{-1} because of stretching of the O–H, carbonyl, and carboxylate groups, respectively. At room temperature, this complex shows a broad ESR signal at $g = 2.18$, a characteristic feature of the copper(II) complex. Generally, hydroxylamine is a reducing agent for copper(II) in basic conditions but in the present reaction condition, it did not cause a reduction. The complex has one 1,10-phenanthroline coordinating to a copper(II) ion, and an in situ formed 4-carboxyphenyloximate as the chelating ligand. The anionic carboxylate end of this ligand neutralizes the overall charge of the complex. The complex has a distorted square pyramidal geometry, where the $d_{\text{Cu–Cl}}$ is 2.613(1) Å. The base of the square pyramid comprises an O2N2 environment. The Cu1–N1 and Cu1–N2 bond distances are 1.989(3), 1.998 (3) Å, respectively, whereas the two Cu–O bond distances, namely, Cu1–O1 is 1.935(3) Å and Cu1–O2 Å is 1.937(3) Å. These distances are comparable to each other. Complex **4** was probably formed by attack of a water molecule on an oxime molecule formed in situ. Such a reaction generated the carboxy-oximate ligand that ligates to the copper(II) ion. Therefore, we have tested this possibility by carrying out the reaction in the presence of isotope labeled water, namely, H_2^{18}O by following an identical reaction procedure used as in the synthesis of complex **4**. As the product **4** obtained is in very small quantity, we examined the products formed in situ by mass spectrometry. To do so, we have analyzed the mass peaks ranging between 160 and 190 of the mass spectra of the samples from two independent experiments; one performed with water and the other with isotopic labeled water. There is a mass peak at 181.0758 because of the 4-(hydroxycarbamoyl)benzoic acid in the mass spectra of each reaction mixture of these two independent reactions. The intensity of the mass peak at 184.1159 is enhanced drastically in the mass spectra of the sample from the reaction mixture where isotopic labeled H_2^{18}O was used (Figure S13). This shows the incorporation of ^{18}O to 4-(hydroxycarbamoyl)benzoic acid whose $m + 1$ value fits to this value of mass. There are established examples where the copper(II) ion-mediated attack of an oxy-solvent on the $\text{C}=\text{N}$ bond of heterocyclic compounds⁷⁴ takes place, but we have difficulty in ascertaining this point in a completely convincing manner in the present case.

4-Formylbenzoate Complex of Cadmium(II). We had earlier suggested that compositions and structures of the cadmium benzoate complexes are highly dependent on the ancillary ligands as well as substituents.⁷⁵ It was also suggested that a poly-nuclear cadmium carboxylate complex may be a polymer in solid state but a monomer in solution.⁷⁶ These happen as a consequence of variable coordination numbers of cadmium ion deciding the respective self-assembly. There are examples of neutral zinc^{54,55} molecular complexes where neutral complexes comprise similar ligands; but, in the present case, two independent compositions are held together by weak noncovalent interactions. Such complexes generate interest to study noncovalently linked self-assemblies of closely related dissimilar complexes. The reaction of cadmium(II) acetate with 4-formylbenzoic acid and 1,10-phenanthroline yielded an unusual molecular complex.

The cadmium complex **5** shown in Figure 3 is an adduct of the mononuclear cadmium complex $[\text{Cd}(\text{phen})(4\text{forben})_2]$ and dinuclear $[\text{Cd}_2(\text{phen})_2(4\text{forben})_4]$ (phen = 1,10-phenanthroline, 4forben = 4-formylbenzoate). The powder XRD pattern of the bulk sample of the complex matches with the

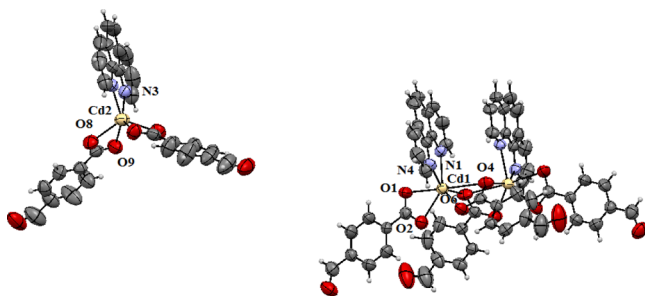


Figure 3. Crystal structure of complex 5

diffraction pattern generated from the CIF file of the complex by using Mercury Software (Figure S1). Hence, it is the only product formed in the reaction. We have re-dissolved the complex independently in different solvents and recrystallized, but we could not get crystals for the two independent components as a single species. The coordination number of cadmium in the dinuclear species is eight; which is six in the mononuclear part. The 1,10-phenanthroline ligands of both the neutral species are bidentate. The dinuclear unit has bidentate chelating formylbenzoate ligands, which also provide μ^1 -bridges to hold cadmium ions. This makes Cd_2O_2 type of linkage by expanding the coordination number of cadmium to eight. Hence, the dinuclear species is a combination of two mononuclear units.

Utility of the Zinc and Cadmium Complex in Sensing of Nitroanilines. Many nitroaromatic compounds are toxic;⁷⁸ hence, their detections at low concentrations by abundant nontoxic metal ions may have utility.¹⁸ Thus, it is necessary to differentiate the ability of detection of nitroaromatic compounds by the nontoxic zinc complex over the cadmium complex as cadmium ions are generally toxic. Furthermore, the zinc–salicylaldehyde complex is able to detect nitroaromatics through photoluminescence quenching.⁸⁰ It suggests that a simple mononuclear zinc complex can serve such a purpose. In fact, there are examples of zinc complexes that detect nitroaromatics.^{80–83} Having these existing facts in mind, complexes with high stability in solution prepared through simple synthetic procedures are essential for their utility as sensors. Furthermore, at ambient conditions, anilines are weak ligands. Hence, a sensing methodology based on weak interactions in the second coordination sphere would be more appropriate.^{82,83} However, there are many examples of metal–organic frameworks showing excellent sensitivity toward nitroaromatics.⁷⁹ The examples of small metal complexes to do so are relatively less.^{15–18} The fluorescence active zinc complex 2 as well as the cadmium complex 5 are structurally simple; they are easily synthesized. In an earlier study, we found that self-assembly of a free pyridine complex was formed by weak interactions of a free pyridine molecule to hold multiple dissimilar nickel complexes.⁸⁴ These entices one to study assemblies of metal complexes to explore their aggregation in solution. Dynamic light scattering (DLS) studies of solutions of the two complexes in dimethylsulphoxide (DMSO) show that they are aggregates in solution (Supporting Information, Figure S17). The particles of the zinc complex and the cadmium complex in DMSO solution have an average size of 338.8 and 380.4 nm, respectively. The respective average particle sizes of the two complexes with 4-nitroaniline are 558.1 and 453.2 nm. Therefore, the aggregation behavior of these complexes

changes in the presence of nitroaniline and there is an increase in sizes in both the cases. The ^1H NMR of complex 5 in solution is similar to the ^1H NMR of the mononuclear zinc(II) complex 2. This suggests that the two neutral species observed in the crystal structure of complex 5 are not distinguishable in solution. The presence of only one species in solution for 5 from ^1H NMR spectra, but observation on the two species with independent Cd-environments in the crystal structure, suggests the possibility of self-association. Definite evidence for aggregation equilibrium comes from the DLS results. The observed particle sizes from the DLS study for both the complexes are larger than the expected molecular weight for a mononuclear complex, showing that aggregation of the complexes takes place in solution. The aggregates formed in solution equilibrate with segregated species with smaller molecular weights. This could be a reason to obtain a mononuclear complex in the case of zinc and self-assembled species in the case of cadmium upon crystallization. In the latter case, the association through expansion of coordination is easy. In an earlier study, the crystal structure of a coordination polymer⁷⁶ of cadmium benzoate confirmed it to be a polymer but it remains as a monomer in solution. This happened because of segregation of the polymeric backbone in solution, by loss of side-on bridges offered by carboxylate ligands.^{76,77} Solvent-dependent aggregation of zinc–benzoate complexes are also known.^{84,85} In the present case, our attempts to get suitable ESI mass of low-molecular-weight complexes were not successful. The aggregation equilibrium is further supported by the fact that when 4-nitroaniline was added, the average particle sizes were increased.

The solution of complex 2 and complex 5 in DMSO emits at 411, 431, and 466 nm upon excitation at 385 nm but with different quantum yields. The ligand 1,10-phenanthroline is also very weakly emitting at those wavelengths, having a quantum yield of 0.030 in DMSO. The quantum yields of the zinc and cadmium complex in DMSO solutions are 0.012 and 0.082, respectively. Complex 2 and complex 5 are soluble in DMSO and dimethyl formamide but not soluble in acetonitrile, methanol, and water. Hence, emission spectra were measured in different mixed solvents to confirm the effect of the solvent to show any solvatoemissive effect. The quantum yields from different emission spectra of the complexes in different mixed solvents in DMSO are listed in Supporting Information Table S1. No shift in emission peaks occurred upon changing solvents except the intensity differences. Both the complexes have the highest respective photoluminescence quantum yield in DMSO. In each case, the cadmium complex showed a relatively higher value of quantum yield than the zinc complex. The emission peaks of the complexes are from the $S_1 \rightarrow S_0$ transition of the 1,10-phenanthroline ligand where the vibrational contributions from $v_0 \rightarrow v_0$, $v_0 \rightarrow v_1$ and $v_0 \rightarrow v_2$ emissions are reflected as three independent but closely spaced emission peaks. Complexes 2 and 5 are metal complexes with d^{10} -electronic configuration but have different ionic radii and electron affinities. Each has π -delocalized 1,10-phenanthroline heterocyclic fluorophore as one of the ligands. Hence, there are possibilities of charge-transfer from the ligand to electron-deficient nitroaromatic compounds. This effect caused quenching of emission of the two complexes upon interactions with nitroanilines. The excimer emissions of cadmium complexes in π -stacked systems modulate emission through stimuli.⁴³ In solution, the emissions of both the complexes get quenched by adding nitroanilines. Two representative cases of

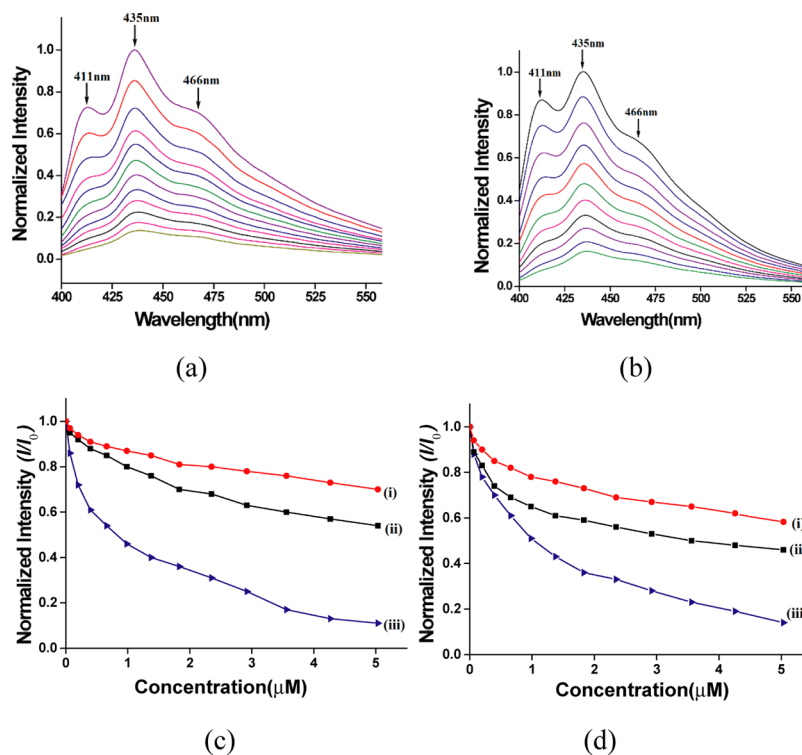


Figure 4. Fluorescence titration (excitation at 385 nm) of (a) complex 2 (10^{-4} M in DMSO) and (b) complex 5 (10^{-4} M in DMSO) with 4-nitroaniline ($20 \mu\text{L}$ aliquot of 10^{-4} M in DMSO). Stern–Volmer plots for (c) complex 2 and (d) complex 5 with (i) 3-nitroaniline, (ii) 2-nitroaniline, and (iii) 4-nitroaniline.

fluorescence quenching of complexes 2 and 5 by 4-nitroaniline are shown in Figure 4a,b, respectively. In each case, the emission of the complex at 411, 435 and 465 nm continuously decreases upon addition of different aliquots of 4-nitroaniline. The emissions decrease in both the complexes being similar but differing in emission intensities suggests a ligand-centered emission where the electronic effects of the metal ions exist. Comparative emission quenching abilities of three isomers of nitroaniline are reflected in the corresponding Stern–Volmer plots shown in Figure 4c,d. Apparently, no significant differences in the decreasing trend caused by the two metal complexes in the ratios of intensity of emission at a particular concentration (I) with respect to initial emission intensity (I_0) as a function of concentrations are observed from as compared to individual nitroaniline. However, the profiles of decreasing emissions of each nitroaniline differ from each other. This makes it clear that the quenching paths of the two metal complexes resemble. The differences in overall effect by the two metal complexes are from the quantum yields of the parent complexes. The cadmium complex has a relatively higher quantum yield but has apparently lower changes in intensities. The nonlinear decay in the value of I/I_0 in each profile as a function of increasing concentrations of respective nitroaniline was observed. Hence, in these detection processes, static quenching occurred, where ground states are not changed. This is also confirmed by carrying out independent ^1H NMR titrations of both the complexes with 4-nitroaniline (Supporting Information Figures S14 and S15). In these titrations, no shift in the chemical shift position of protons of the complexes or the 4-nitroaniline occurred. To understand the quenching paths, the emission spectra of 1,10-phenanthroline and 4-formylbenzoic acid (385 nm excitation) were independently recorded. Both these compounds emit very weakly. The 1,10-

phenanthroline weakly emits at 411, 435, and 465 nm, whereas the 4-formylbenzoic acid emits at 412 and 436 nm (Supporting Information Figure S19). The emission at 430 nm of 4-formylbenzoic acid upon addition of an equivalent amount of zinc(II) chloride causes an increase in intensity and resulted in emission to complex 2. Addition of 4-nitroaniline to such a solution decreases the emission intensity. The 1,10-phenanthroline also showed a similar trend and the observations are apparently similar irrespective of the ligand or zinc or cadmium complex used in sensing. Control experiments on emission of 1,10-phenanthroline in solution upon addition of cadmium(II) chloride also provided similar observations; but differences in these experiments are the relative changes in the emission intensities. The results suggest a synergic electronic effect between the ligands mediated by the d^{10} -metal ions but this effect is not a dominant in quenching. The d^{10} -metal ions provide a template to push electron density, enhancing the transition probability of the weakly fluorescent ligand. From the crystal structures, it is also clear that the aggregations of the two complexes differ; but there is equilibration among the low-molecular-weight species in solution; hence the emission wavelengths are at the same place for both the complexes. Solid samples of complex 2 and complex 5 have broad emission at 465 nm ($\lambda_{\text{ex}} = 385$ nm) and the cadmium complex has a higher intensity. The copper(II) complexes are nonfluorescent because of fluorophore directly connected to the paramagnetic copper(II) ion. The crystal structures of the zinc complexes have C–H $\cdots\pi$ and C–H $\cdots\text{O}$ interactions in self-assembly (Figure S16). However, the cadmium complex has extensive parallel co-facial π -stacking among the phenanthroline rings in solid state and the two neutral complexes are held in the lattice together by C–H $\cdots\text{O}$ interactions illustrated in Supporting Information Figure S17. The solid samples of

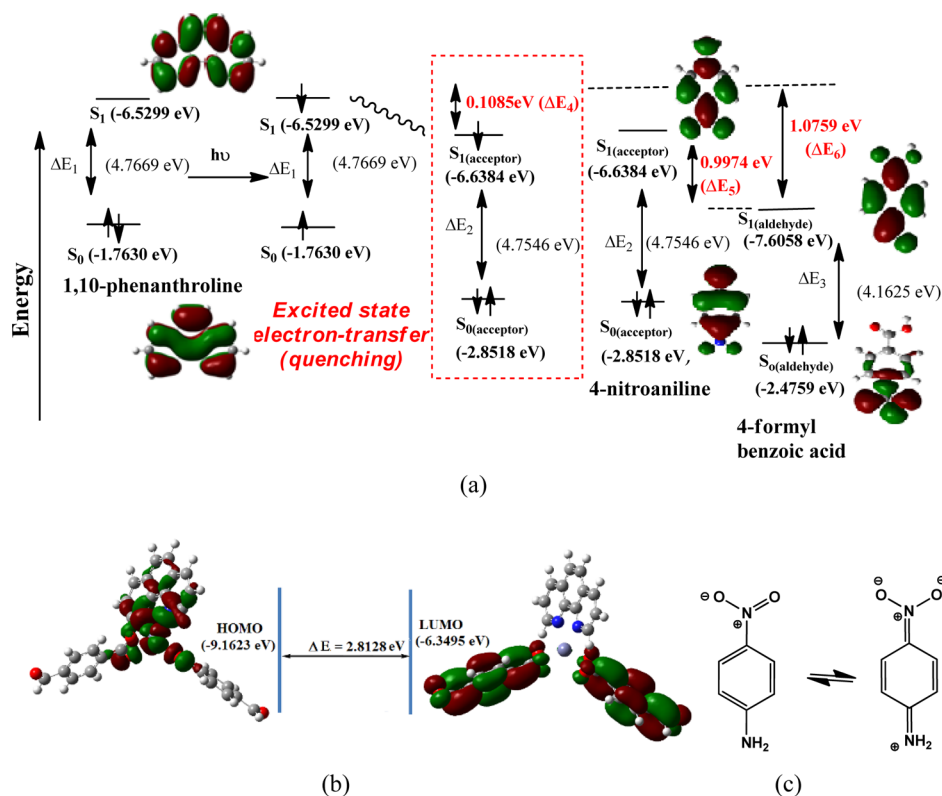


Figure 5. (a) Plausible quenching paths based on quenching of emission of 1,10-phenanthroline; (b) HOMO–LUMO of the zinc complex (2) calculated by Gaussian software using the B3LYP functional and the 6-31 + G (d,p) basis set; (c) resonance structures of 4-nitroaniline.

the two complexes showed a triexponential emission decay profile in each case. The emission decay profile of the cadmium complex has equal distribution over those three paths. Among them, two paths have relatively short lifetimes, whereas 38.8% molecules follow a path of a relatively longer lifetime of 13.36 ns. The zinc complex has two short-lifetime paths by smaller fractions of molecules, and the major portions comprising 72.83% of molecules follow a slightly longer path of lifetime of 4.97 ns (Supporting Information Figures S11 and S12). The differences in the number of fractions of the longer lifetimes are indicative of the fractions of excimer-like emissions in the two cases because of packing differences. The cadmium complex has extensive parallel co-facial π -stacks, whereas the zinc complex has C–H $\cdots\pi$ interactions; these interactions provide definite arrangements to the fluorophores, which also contribute to the decay path with a longer lifetime.

As the ligand 1,10-phenanthroline itself shows a similar quenching process and similar emission as that of the complexes, a plausible mechanism shown in Figure 5a is proposed for the observed quenching based on the electronic levels of the ligands; a similar explanation is also applicable to metal complexes. Density functional theory (DFT) optimization of energies [using B3LYP functional and 6-31+G (d,p) basis set] of 1,10-phenanthroline and 4-nitroaniline show that the lowest unoccupied molecular orbital (LUMO) of 1,10-phenanthroline has slightly higher energy than the LUMO of the 4-nitroaniline ($\Delta E_4 = 0.1085$ eV). Upon excitation, an electron from S_0 of the 1,10-phenanthroline is excited to the S_1 state. As the difference of LUMOs of the donor 1,10-phenanthroline and the acceptor 4-nitroaniline is small, the excited electron from the LUMO of the 1,10-phenanthroline is transferred easily to the LUMO of the 4-nitroaniline. This

results in the quenching through excited-state charge transfer. The LUMO of aldehyde has substantial differences from the energy than the LUMO of 4-formylbenzoic acid ($\Delta E_5 = 0.9974$ eV), whereas the energy difference between the respective LUMO of 4-nitroaniline and 4-formylbenzoic acid (ΔE_6) is 1.0759 eV. Nitroanilines quench fluorescence of perylene-based receptors,⁸⁶ enabling differentiation of positional isomers in a similar manner that we have observed with the present examples. The energy of the zinc complex is optimized by Gaussian software using the B3LYP functional and the 6-31+G (d,p) basis set. The highest occupied molecular orbital (HOMO)–LUMO are presented in Figure 5b, indicating that the HOMO is localized in the 1,10-phenanthroline ring whereas the LUMO is localized over the 4-formylbenzoate unit. The HOMO–LUMO energy gap in the zinc complex (2) is 2.812 eV (440.9 nm). This clearly indicates that an S_0 – S_1 excitation involves charge transfer from the donor site to the acceptor site of the complex and shows that there exists a push–pull path mediated by the intervening d^{10} metal ions, which is anchoring the ligands having inherent electron-withdrawing and -releasing properties. Thus, exciplex formation of the nitroanilines with the metal complexes inhibited the excited electron to retrace the original path to the ground state of those complexes.

Among the three positional isomers, the highest quenching was caused by 4-nitroaniline. It is 35-fold higher than the corresponding emission quenching caused on the zinc complex by the meta-isomer. The ortho-isomer has 2.5-times higher quenching ability than the meta-isomer. The higher quenching ability of 4-nitroaniline is attributed to the resonance forms of nitroaniline and iminoquinone structures shown in Figure 5c.

The non-aromatic electron-deficient nature of the imino-quinone makes it a better acceptor for efficient quenching.

The detection limits for the three positional isomers of nitroaniline determined from the fluorescence titrations are listed in Table 1. These show that the zinc(II) complex has a

Table 1. Detection Limits ($3\sigma/k$) of the Three Positional Isomers of Nitroaniline

compound	detection limit (μM)	
	zinc complex	cadmium complex
4-nitroaniline	0.38	0.50
2-nitroaniline	0.43	1.15
3-nitroaniline	0.67	1.59

superior detection limit over the cadmium complexes for the three isomers. The 2-amino-5-nitrophenol (Figure S7) is also an excellent quencher of the two complexes. These results complement the quenching of emission through $\text{O}\cdots\pi$ interactions on cobalt(II)¹⁷ and nickel(II)¹⁸ 1,10-phenanthroline complexes responsible in photoluminescence quenching by nitroaromatic compounds. The present complexes have the advantages of having simple structures and are readily soluble in DMSO and dimethylformamide (DMF); they are also easily synthesized from commercially available reagents. Though the present system is based on a relatively low quantum yield, their scopes exist to develop more improvised system based on transition-metal complexes based on the foundations provided here.

CONCLUSIONS

The reactivity and sensing of structurally simple complexes of the 1,10-phenanthroline ligand containing copper, zinc, and cadmium 4-formylbenzoate complexes are depicted. The study provided the fundamental understanding on the quenching of emission of 1,10-phenanthroline and the two d^{10} metal ion complexes to be through the transfer of excited from excited state to the nitroanilines. The possible push–pull electronic effects of the donor and acceptor ligands are reflected in the theoretically demonstrated zinc complex where the LUMO is localized on the 1,10-phenanthroline ligand, whereas LUMO is localized at the 4-formylbenzoate part. Besides all these structural aspects, an unusual molecular complex of cadmium is also serendipitously isolated and characterized. This complex has two neutral cadmium complexes self-assembled through $\text{C}-\text{H}\cdots\pi$ and $\text{C}-\text{H}\cdots\text{O}$ interactions. The DLS experiments have shown that the zinc and cadmium complexes form aggregates in solution and the particle sizes of such aggregates are increased upon interactions with nitroaniline. Both those complexes are useful in the efficient detection of nitroanilines. The paramagnetic copper complexes studied in this study are unsuitable for fluorescence detection of analytes, but they provided fundamental understandings on the reactivity of hydroxylamine, which is a conventional volatile pollutant and mild reducing agent. The packing pattern determined from the crystal structure of a copper(II) formylbenzoate complex possesses complex cations encapsulated in self-assembly of oximes with hydrated-chloride ions. The packing of the complex does not have direct interactions between oxime and carboxylic acid but hydrated-chloride ions provided the charge-assisted hydrogen bonds with the oxime functional

Table 2. Crystallographic Parameters of Complexes 1–5

parameters	complex 1	complex 2	complex 3	complex 4	complex 5
formula	$\text{C}_{28}\text{H}_{20}\text{Cu}_1\text{N}_2\text{O}_7\text{Cu}$	$\text{C}_{28}\text{H}_{18}\text{N}_2\text{O}_6\text{Zn}$	$\text{C}_{40}\text{H}_{34}\text{N}_6\text{Cl}_2\text{O}_8\text{Cu}$	$\text{C}_{20}\text{H}_{22}\text{N}_3\text{Cl}_1\text{O}_8\text{Cu}$	$\text{C}_{84}\text{H}_{54}\text{N}_6\text{O}_{18}\text{Cd}_3$
CCDC	1943593	1943596	194395	194394	194397
mol. wt.	560.00	543.81	861.17	531.39	1772.53
space group	$P\bar{1}$	$P2_1/n$	$I2/a$	$P2_1/c$	$P2_12_12$
a (Å)	7.8659(5)	7.6269(2)	13.6241(5)	13.3912(13)	16.1308(5)
b (Å)	10.7334(5)	18.8777(6)	19.7951(9)	13.7749(9)	23.6787(7)
c (Å)	15.3411(9)	16.9569(6)	15.5784(6)	13.1200(16)	9.7385(3)
α (deg)	102.735(5)	90	90	90.00	90
β (deg)	93.637(5)	101.225(2)	107.568(4)	116.239(14)	90
γ (deg)	107.559(5)	90	90	90.00	90
V (Å ³)	1192.68(12)	2394.72(13)	4005.4(3)	2170.8(4)	3719.7(2)
density, g cm^{-3}	1.559	1.508	1.428	1.626	1.583
Abs. coeff., mm^{-1}	0.969	1.074	0.738	1.183	0.927
$F(000)$	574	1112	1772	1092	1776
total no. of reflections	4317	4237	3548	3847	6576
reflections, $I > 2\sigma(I)$	3705	2980	2765	3245	5552
max. θ/deg	25.245	25.05	25.05	25.047	25.048
ranges (h, k, l)	$-9 \leq h \leq 9$ $-12 \leq k \leq 12$ $-13 \leq l \leq 18$	$-9 \leq h \leq 9$ $-21 \leq k \leq 22$ $-20 \leq l \leq 19$	$-16 \leq h \leq 15$ $-13 \leq k \leq 23$ $-18 \leq l \leq 18$	$-15 \leq h \leq 15$ $-15 \leq k \leq 16$ $-15 \leq l \leq 15$	$-18 \leq h \leq 19$ $-28 \leq k \leq 27$ $-11 \leq l \leq 11$
complete to 2θ (%)	99.8	100.0	99.9	99.9	99.7
data/restraints/parameters	4317/3/348	4237/0/334	3548/1/269	3847/5/333	6576/0/501
GooF (F^2)	1.070	1.086	1.004	1.072	1.245
R indices [$I > 2\sigma(I)$]	0.0678	0.0393	0.0450	0.0485	0.0310
wR_2 [$I > 2\sigma(I)$]	0.1796	0.0945	0.1339	0.1299	0.0413
R indices (all data)	0.0767	0.0643	0.0633	0.0583	0.0422
wR_2 (all data)	0.1870	0.1052	0.1556	0.1360	0.0429

group to form an assembly. Such an assembly assisted by water molecules has a direct implication on understanding a way of formation of water-mediated aggregation of anions with neutral components. Beyond those results, an exceptional copper 4-(hydroxycarbamoyl)benzoate complex is isolated and characterized from the copper(II)-mediated oximation reaction, which has a definite role in further developing chemosensing properties to detect volatile organic compounds, more precisely hydroxylamine hydrochloride.

EXPERIMENTAL SECTION

General. Infrared spectra of the solid samples were recorded on a PerkinElmer Spectrum One FT-IR spectrophotometer by making KBr pellets. Powder XRD patterns were recorded using a Bruker powder X-ray diffractometer D2 phaser instrument. ^1H NMR spectra were recorded on a BRUKER Ascend-600 MHz NMR spectrometer using TMS as the internal standard. A PerkinElmer LAMDA-750 spectrometer was used to record the solid-state UV–visible spectra by diffuse reflectance. Fluorescence emissions were measured in a Horiba Jobin Yvon FluoroMax-4 spectrofluorometer by taking definite amount of solutions or definite amounts of the solid sample and exciting at the required wavelength. Electron paramagnetic resonance spectra were recorded on a JES-FA200 ESR spectrometer at room temperature, with a microwave power of 0.998 mW, microwave frequency of 9.14 GHz, and modulation amplitude of 2. DLS experiments were carried out on a Malvern Zeta sizer Nano ZS instrument equipped with a 4.0 mW He–Ne laser operating at 633 nm.

The detection limits for the positional isomers of nitroaniline were calculated from the formula: detection limit = $3\sigma/k$, where σ is the standard deviation in blank measurements and k is the slope from the plot between the fluorescence emission intensity against concentration of the respective nitroaniline. For such measurements, the fluorescence emission spectra of complex 2 and complex 5 were measured 10 times and the standard deviation of the measurements was determined. The slope was obtained from the independent plot of intensity of emission at 435 nm of the complex versus concentration of the respective nitroaniline. The quantum yields in solutions were determined from the integrated areas of emission based on quinine sulphate as the standard.

Crystallographic Study. Single-crystal XRD data for complexes 2 and 5 were collected at 296 K with Mo $K\alpha$ radiation ($\lambda = 0.71073 \text{ \AA}$) by a Bruker Nonius SMART APEX CCD diffractometer equipped with a graphite monochromator and an Apex CCD camera, whereas data for complex 1, 3, and 4 were collected on an Oxford SuperNova diffractometer. Data reductions and cell refinement for data obtained from an Oxford diffractometer were performed by CrysAlisPro software and from a Bruker Nonius diffractometer were performed using SAINT and XPREP software. Structures were solved by a direct method and were refined by full-matrix least-squares on F^2 using SHELXL-2014 software. All nonhydrogen atoms were refined in anisotropic approximation against F^2 of all reflections. The hydrogen atoms were placed at their geometric positions by riding and refined by isotropic approximation. From the data collected at room temperature the disorder of the oxygen atoms of the aldehydes in complex 1 and short contacts between two hydrogen atoms of molecules of water of crystallization in the structure of complex 4 could not be resolved. The crystallographic parameters of the complexes are listed in Table 2.

Synthesis and Characterization. (1,10-Phenanthroline)-bis(4-formylbenzoate)(aqua)copper(II) (1). To a well-stirred solution of 4-formyl benzoic acid (300 mg, 2.0 mmol) and 1,10-phenanthroline (99 mg, 0.5 mmol) in methanol, copper(II) acetate monohydrate (199 mg, 1 mmol) was added. The resulting solution was stirred for about 4 h. The precipitate formed was dissolved in water and the resulting solution was kept undisturbed for crystallization. Dark-blue crystals appeared after 2 days. (Isolated yield: 59%). IR (KBr, cm^{-1}): 3439 (br, w), 1692 (s), 1595 (s), 1558 (w), 1520 (s), 1498 (s), 1436 (w), 1426 (s), 1385 (s), 1261 (m), 1203 (s), 1130 (m), 1106 (m), 841 (s), 802 (s).

(1,10-Phenanthroline)bis(4-formylbenzoate)zinc(II) (2). The zinc complex 2 was synthesized in an identical procedure as that of complex 1, but in this case dimethylacetamide was used as solvent, and zinc(II) acetate dihydrate (219 mg, 1 mmol) was used instead of copper(II) acetate. Upon crystallization, dirty-white crystals of complex 2 were isolated in 67% yield. ^1H NMR (600 MHz, $\text{DMSO-}d_6$): 10.01 (s, 2H), 9.21 (s, 2H), 8.87 (d, $J = 6 \text{ Hz}$, 2H), 8.25 (s, 2H), 8.08 (m, 6H), 7.87 (d, $J = 6 \text{ Hz}$, 4H). IR (KBr, cm^{-1}): 3439 (br, w), 3060 (m), 1702 (s), 1643 (s), 1598 (s), 1552 (s), 1519 (m), 1505 (s), 1401 (s), 1299 (s), 1202 (s), 1134 (s), 1105 (m), 1013 (s), 869 (s), 853 (s), 819 (s).

Inclusion Complex of Bis(1,10-phenanthroline)(chloro)copper(II) Chloride with 4-((Hydroxyimino)methyl) Benzoic Acid (3). To a well-stirred solution of 4-formylbenzoic acid (300 mg, 2 mmol), 1,10-phenanthroline (99 mg, 0.50 mmol) and hydroxylamine hydrochloride (138 mg, 2 mmol) in methanol, copper(II) acetate monohydrate (199 mg, 1 mmol) was added. After stirring for 4 h, the precipitate formed was re-dissolved by adding water (20 mL) to make a homogeneous solution. The solution on standing yielded dark-blue crystals of copper complex 3 in 71% yield. IR (KBr, cm^{-1}): 3395 (br, s), 1688 (s), 1651 (m), 1518(s), 1427 (s), 1343 (m), 1313 (m), 1277 (s), 1217 (m), 1177 (m), 1145 (w), 1177 (m), 1107 (m), 1016 (m), 946 (s), 876 (m), 853 (s).

Copper(II) Complex of 4-(Hydroxycarbamoyl)benzoic Acid (4). It was prepared in a similar procedure as that of complex 3; but in this case the hydroxylamine was generated for the reaction in situ by adding sodium acetate. A solution of 4-formylbenzoic acid (300 mg, 2 mmol) and 1,10-phenanthroline (99 mg, 0.5 mmol) in methanol, copper(II) acetate monohydrate (199 mg, 1 mmol) was reacted with hydroxylamine hydrochloride (690 mg, 10 mmol). To this solution, sodium acetate (500 mg, 6 mmol) was added; the solution turned from green to red and finally to a dark-blue color. The precipitate formed was dissolved in water (10 mL) and kept undisturbed for crystallization. Few dark-blue crystals of complex 4 were obtained from a mixture of crystals. The other crystals were not of good diffracting quality, and upon recrystallization from DMF gave crystals of bis(1,10-phenanthroline)(chloro)copper(II) chloride. DMF (confirmed by comparing by single-crystal XRD)³⁴ and remaining residue upon purification yielded the oxime. The isolated yield of complex 4 is 6%. IR (KBr, cm^{-1}): 3403 (br, s), 1721 (s), 1679 (s), 1629 (w), 1598 (s), 1521 (s), 1493 (m), 1429 (s), 1367 (w), 1306 (m), 1279 (s), 1177 (m), 1148 (s), 1109 (s), 1029 (s), 1013 (m), 918 (s), 873 (s), 851 (s).

Molecular Complex of (1,10-Phenanthroline)bis(4-formylbenzoate)cadmium(II) (5). The cadmium complex 4 was prepared by an identical procedure as that of zinc complex 2 but cadmium(II) acetate dihydrate (266 mg, 1 mmol) was

used instead of zinc(II) acetate in methanol (20 mL). Dirty-white crystals were collected. Isolated yield: 65%. ^1H NMR (600 MHz, DMSO- d_6): 10.01 (s, 6H), 9.19 (s, 6H), 8.80 (d, J = 12 Hz, 6H), 8.09 (s, 6H), 8.19–8.04 (m, 18H), 7.89 (d, J = 6 Hz, 12H). IR (KBr, cm^{-1}): 3439 (br, m), 1700 (s), 1689 (s), 1621 (s), 1593 (s), 1552 (s), 1515 (s), 1500 (s), 1426 (m), 1403 (s), 1296 (m), 1205 (s), 1143 (s), 1101 (s), 1049 (w), 1013 (s), 856 (s), 814 (s).

■ ASSOCIATED CONTENT

● Supporting Information

The Supporting Information is available free of charge on the ACS Publications website at DOI: 10.1021/acsomega.9b02779.

^1H NMR spectra of the zinc and cadmium complexes, ^1H NMR titration, hydrogen-bonds table, fluorescence titrations, DLS plots, and quantum yields (PDF)

Crystallographic information files of complexes 1–5 (CIF)

■ Accession Codes

The CIF files of the complexes are deposited to CCDC, having the numbers 1943593, 1943594, 1943595, 1943596, and 1943597.

■ AUTHOR INFORMATION

■ Corresponding Author

*E-mail: juba@iitg.ac.in. Phone: +91-361-2582311. Fax: +91-361-2690762.

■ ORCID

Jubaraj B. Baruah: 0000-0003-3371-7529

■ Notes

The authors declare no competing financial interest.

■ ACKNOWLEDGMENTS

The authors thank the Ministry of Human Resources and Development, Government of India, New Delhi, for financial support through a departmental grant (no. F. no. 5-1/2014-TS.VII).

■ REFERENCES

- (1) Wong, K. M.-C.; Chan, M. M.-Y.; Yam, V. W.-W. Supramolecular Assembly of Metal-Ligand Chromophores for Sensing and Phosphorescent OLED Applications. *Adv. Mater.* **2014**, *26*, 5558–5568.
- (2) Wieczorek, B.; Dijkstra, H. P.; Egmond, M. R.; Klein Gebbink, R. J. M.; van Koten, G. Incorporating ECE-pincer metal complexes as functional building blocks in semisynthetic metalloenzymes, supramolecular polypeptide hybrids, tamoxifen derivatives, biomarkers and sensors. *J. Organomet. Chem.* **2009**, *694*, 812–822.
- (3) Korybut-Daszkiewicz, B.; Bilewicz, R.; Woźniak, K. Tetraimine macrocyclic transition metal complexes as building blocks for molecular devices. *Coord. Chem. Rev.* **2010**, *254*, 1637–1660.
- (4) Panunzi, B.; Concilio, S.; Diana, R.; Shikler, R.; Nabha, S.; Piotto, S.; Sessa, L.; Tuzi, A.; Caruso, U. Photophysical properties of luminescent zinc(II)-pyridinylloxadiazole complexes and their glassy self-assembly networks. *Eur. J. Inorg. Chem.* **2018**, *2018*, 2709–2716.
- (5) Panunzi, B.; Borbone, F.; Capobianco, A.; Concilio, S.; Diana, R.; Peluso, A.; Piotto, S.; Tuzi, A.; Velardo, A.; Caruso, U. Synthesis, spectroscopic properties and DFT calculations of a novel multipolar azo dye and its zinc(II) complex. *Inorg. Chem. Commun.* **2017**, *84*, 103–108.

- (6) Ma, D.-L.; Ma, V. P.-Y.; Chan, D. S.-H.; Leung, K.-H.; He, H.-Z.; Leung, C.-H. Recent advances in luminescent heavy metal complexes for sensing. *Coord. Chem. Rev.* **2012**, *256*, 3087–3113.

- (7) Strianese, M.; Pellecchia, C. Metal complexes as fluorescent probes for sensing biologically relevant gas molecules. *Coord. Chem. Rev.* **2016**, *318*, 16–28.

- (8) Kumar, S.; Kishan, R.; Kumar, P.; Pachisia, S.; Gupta, R. Size-selective detection of picric acid by fluorescent palladium macrocycles. *Inorg. Chem.* **2018**, *57*, 1693–1697.

- (9) Chhatwal, M.; Mittal, R.; Gupta, R. D.; Awasthi, S. K. Sensing ensembles for nitroaromatics. *J. Mater. Chem. C* **2018**, *6*, 12142–12158.

- (10) Berezin, A. S.; Samsonenko, D. G.; Brel, V. K.; Artem'ev, A. V. "Two-in-one" organic-inorganic hybrid MnII complexes exhibiting dual-emissive phosphorescence. *Dalton Trans.* **2018**, *47*, 7306–7315.

- (11) Liu, J.-W.; Xu, Y.-N.; Qin, C.-Y.; Wang, Z.-N.; Wu, C.-J.; Li, Y.-H.; Wang, S.; Zhang, K. Y.; Huang, W. Simple fluorene oxadiazole-based Ir (III) complexes with AIPE properties: synthesis, explosive detection and electroluminescence studies. *Dalton Trans.* **2019**, *48*, 13305–13314.

- (12) Zhang, S.; Yuan, W.; Qin, Y.; Zhang, J.; Lu, N.; Liu, W.; Li, H.; Wang, Y.; Li, Y. Bidentate BODIPY-appended 2-pyridylimidazo[1,2-a]pyridine ligand and fabrication of luminescent transition metal complexes. *Polyhedron* **2018**, *148*, 22–31.

- (13) Shamsieva, A. V.; Musina, E. I.; Gerasimova, T. P.; Fayzullin, R. R.; Kolesnikov, I. E.; Samigullina, A. I.; Katsyuba, S. A.; Karasik, A. A.; Sinyashin, O. G. Intriguing near-infrared solid-state luminescence of binuclear silver(I) complexes based on pyridylphospholane scaffolds. *Inorg. Chem.* **2019**, *58*, 7698–7704.

- (14) Sathish, V.; Ramdass, A.; Velayudham, M.; Lu, K.-L.; Thanasekaran, P.; Rajagopal, S. Development of luminescent sensors based on transition metal complexes for the detection of nitro-explosives. *Dalton Trans.* **2017**, *46*, 16738–16769.

- (15) Shanmugaraju, S.; Mukherjee, P. S. π -Electron rich small molecule sensors for the recognition of nitroaromatics. *Chem. Commun.* **2015**, *51*, 16014–16032.

- (16) Khullar, S.; Singh, S.; Das, P.; Mandal, S. K. Luminescent lanthanide-based probes for the detection of nitroaromatic compounds in water. *ACS Omega* **2019**, *4*, 5283–5292.

- (17) Shankar, K.; Baruah, J. B. Tetranuclear Cobalt Complexes as Nano-Dimensional Template for Inclusion of Nitrophenols. *ChemistrySelect* **2016**, *1*, 5152–5158.

- (18) Shankar, K.; Baruah, J. B. Mixed anionic and inclusion complexes of nickel(II) with nitroaromatics showing selectivity in oxygen- π interactions. *Inorg. Chim. Acta* **2016**, *453*, 135–141.

- (19) Tarai, A.; Baruah, J. B. Study on divalent copper, nickel and zinc model complexes for fluoride ion detection. *RSC Adv.* **2015**, *5*, 82144–82152.

- (20) Kukushkin, V. Y.; Pombeiro, A. J. L. Oxime and oximate metal complexes: unconventional synthesis and reactivity. *Coord. Chem. Rev.* **1999**, *181*, 147–175.

- (21) Fabbrizzi, L.; Licchelli, M.; Mosca, L.; Poggi, A. Template synthesis of azacyclam metal complexes using primary amides as locking fragments. *Coord. Chem. Rev.* **2010**, *254*, 1628–1636.

- (22) Costisor, O. *Metal Mediated Template Synthesis of Ligands*; World Scientific: Singapore, 2004.

- (23) Ahumada, G.; Oyarce, J.; Roisnel, T.; Kahlal, S.; del Valle, M. A.; Carrillo, D.; Saillard, J.-Y.; Hamon, J.-R.; Manzur, C. Synthesis, structures, electrochemical and quantum chemical investigations of Ni(II) and Cu(II) complexes with a tetradentate Schiff base derived from 1-(2-thienyl)-1,3-butanedione. *New J. Chem.* **2018**, *42*, 19294–19304.

- (24) Lukehart, C. M. Metalla- β -diketones and their derivatives. *Acc. Chem. Res.* **1981**, *14*, 109–116.

- (25) Crowley, J. D.; Goldup, S. M.; Lee, A.-L.; Leigh, D. A.; McBurney, R. T. Active metal template synthesis of rotaxanes, catenanes and molecular shuttles. *Chem. Soc. Rev.* **2009**, *38*, 1530–1541.

- (26) Curtis, N. F. Macrocyclic coordination compounds formed by condensation of metal-amine complexes with aliphatic carbonyl compounds. *Coord. Chem. Rev.* **1968**, *3*, 3–47.
- (27) Fenton, D. E.; Rossi, G. Metal complexes of Schiff base macrocycles having present pendant arms bearing ligating groups. *Inorg. Chim. Acta* **1985**, *98*, L29–L30.
- (28) Adams, H.; Bailey, N. A.; Fenton, D. E.; Fukuhara, C.; Hellier, P. C.; Hempstead, P. D. Dalton communications. Synthesis and crystal structure of a disilver(I) complex of a tetraimine Schiff-base macrocycle having N-isopropylidene-bearing pendant arms. *Dalton Trans.* **1992**, 729–730.
- (29) Dhal, P. K.; Arnold, F. H. Template-mediated synthesis of metal-complexing polymers for molecular recognition. *J. Am. Chem. Soc.* **1991**, *113*, 7418–7420.
- (30) Menon, S. K.; Guha, T. B.; Agrawal, Y. K. Catenanes: template synthesis and application of their metal complexes. *Rev. Inorg. Chem.* **2004**, *24*, 97–133.
- (31) Goldup, S. M.; Leigh, D. A.; Lusby, P. J.; McBurney, R. T.; Slawin, A. M. Z. Gold(I)-template catenane and rotaxane synthesis. *Angew. Chem., Int. Ed.* **2008**, *47*, 6999–7003.
- (32) Nath, J. K.; Kirillov, A. M.; Baruah, J. B. Unusual solvent-mediated hydrolysis of dicarboxylate monoester ligands in copper(II) complexes toward simultaneous crystallization of new dicarboxylate derivatives. *RSC Adv.* **2014**, *4*, 47876–47886.
- (33) Cohen, S. M. Postsynthetic Methods for the Functionalization of Metal-Organic Frameworks. *Chem. Rev.* **2012**, *112*, 970–1000.
- (34) Newkome, G. R.; Shreiner, C. D. Poly(amidoamine), polypropylenimine, and related dendrimers and dendrons possessing different 1→2 branching motifs: An overview of the divergent procedures. *Polymer* **2008**, *49*, 1–173.
- (35) Knecht, M. R.; Wright, D. W. Amine-terminated dendrimers as biomimetic templates for silica nanosphere formation. *Langmuir* **2004**, *20*, 4728–4732.
- (36) Dau, P. V.; Tanabe, K. K.; Cohen, S. M. Functional group effects on metal-organic framework topology. *Chem. Commun.* **2012**, *48*, 9370–9372.
- (37) Collins, S. P.; Daff, T. D.; Piotrkowski, S. S.; Woo, T. K. Materials design by evolutionary optimization of functional groups in metal-organic frameworks. *Sci. Adv.* **2016**, *2*, No. e1600954.
- (38) Li, W.; Li, S. CO₂ adsorption performance of functionalized metal-organic frameworks of varying topologies by molecular simulations. *Chem. Eng. Sci.* **2018**, *189*, 65–74.
- (39) Subudhi, S.; Rath, D.; Parida, K. M. A mechanistic approach towards the photocatalytic organic transformations over functionalised metal organic frameworks: A review. *Catal. Sci. Technol.* **2018**, *8*, 679–696.
- (40) Das, P.; Mandal, S. K. Understanding the effect of an amino group on the selective and ultrafast detection of TNP in water using fluorescent organic probes. *J. Mater. Chem. C* **2018**, *6*, 3288–3297.
- (41) Xi, F.-G.; Liu, H.; Liu, H.; Yang, N.-N.; Gao, E.-Q. Aldehyde-tagged zirconium metal–organic frameworks: a versatile platform for post synthetic modification. *Inorg. Chem.* **2016**, *55*, 4701–4703.
- (42) Mani, P.; Gao, A. A.; Reddy, V. S.; Mandal, S. “Turn-on” fluorescence sensing and discriminative detection of aliphatic amines using a 5-fold-interpenetrated coordination polymer. *Inorg. Chem.* **2017**, *56*, 6772–6775.
- (43) Yan, Y.; Chen, J.; Zhang, N.-N.; Wang, M.-S.; Sun, C.; Xing, X.-S.; Li, R.; Xu, J.-G.; Zheng, F.-K.; Guo, G.-C. Grinding size-dependent mechanoresponsive luminescent Cd(II) coordination polymer. *Dalton Trans.* **2016**, *45*, 18074–18078.
- (44) Baruah, J. B. Predominantly ligand guided non-covalently linked assemblies of inorganic complexes and guest inclusion. *J. Chem. Sci.* **2018**, *130*, 56.
- (45) You, L.; Berman, J. S.; Anslyn, E. V. Dynamic multi-component covalent assembly for the reversible binding of secondary alcohols and chirality sensing. *Nat. Chem.* **2011**, *3*, 943–948.
- (46) Feng, Q.; Wang, M.; Dong, B.; He, J.; Xu, C. Regulation of arrangements of pyrene fluorophores via solvates and cocrystals for fluorescence modulation. *Cryst. Growth Des.* **2013**, *13*, 4418–4427.
- (47) Hinoue, T.; Shigenoi, Y.; Sugino, M.; Mizobe, Y.; Hisaki, I.; Miyata, M.; Tohnai, N. Regulation of π -Stacked Anthracene Arrangement for Fluorescence Modulation of Organic Solid from Monomer to Excited Oligomer Emission. *Chem.—Eur. J.* **2012**, *18*, 4634–4643.
- (48) Li, R.; Wang, S.-H.; Liu, Z.-F.; Chen, X.-X.; Xiao, Y.; Zheng, F.-K.; Guo, G.-C. An Azole-Based Metal-Organic Framework toward Direct White-Light Emissions by the Synergism of Ligand-Centered Charge Transfer and Interligand π - π Interactions. *Cryst. Growth Des.* **2016**, *16*, 3969–3975.
- (49) Shankar, K.; Kirillov, A. M.; Baruah, J. B. A modular approach for molecular recognition by zinc dipicolinate complexes. *Dalton Trans.* **2015**, *44*, 14411–14423.
- (50) Grabowski, Z. R.; Rotkiewicz, K. Structural changes accompanying intramolecular electron transfer: focus on twisted charge-transfer states and structures. *Chem. Rev.* **2003**, *103*, 3899–4031.
- (51) Rettig, K. D.; Makwana, B. A.; Vyas, D. J.; Mishra, D. R.; Jain, V. K. Selective recognition by novel calix system: ICT based chemosensor for metal ions. *J. Lumin.* **2014**, *146*, 450–457.
- (52) Chakrabarty, R.; Mukherjee, P. S.; Stang, P. J. Supramolecular coordination: self-assembly of finite two- and three-dimensional ensembles. *Chem. Rev.* **2011**, *111*, 6810–6918.
- (53) Chen, L.; Chen, Q.; Wu, M.; Jiang, F.; Hong, M. Controllable coordination-driven self-assembly: from discrete metal cages to infinite cage-based frameworks. *Acc. Chem. Res.* **2015**, *48*, 201–210.
- (54) Karmakar, A.; Sarma, R. J.; Baruah, J. B. Self-assembly of neutral dinuclear and trinuclear zinc-benzoate complexes. *Inorg. Chem. Commun.* **2006**, *9*, 1169–1172.
- (55) Phukan, N.; Baruah, J. B. A supramolecular assembly and complexes of zinc 2-hydroxy-3-naphthoate. *RSC Adv.* **2013**, *3*, 1151–1157.
- (56) Singh, D.; Baruah, J. B. Hydroxy-carboxylates of manganese, zinc and cadmium. *Inorg. Chim. Acta* **2013**, *394*, 703–709.
- (57) Deka, K.; Laskar, M.; Baruah, J. B. Carbon-nitrogen bond cleavage by copper(II) complexes. *Polyhedron* **2006**, *25*, 2525–2529.
- (58) Dey, B.; Saha, R.; Mukherjee, P. A luminescent-water soluble inorganic co-crystal for a selective pico-molar range arsenic(III) sensor in water medium. *Chem. Commun.* **2013**, *49*, 7064–7066.
- (59) Chou, C.-C.; Su, C.-C.; Yeh, A. Mononuclear and dinuclear copper(I) complexes of bis(3,5-dimethyl pyrazol-1-yl)methane: synthesis, structure, and reactivity. *Inorg. Chem.* **2005**, *44*, 6122–6128.
- (60) Dai, J.-X.; Wu, F.-H.; Yao, W.-R.; Zhang, Q.-F. One-dimensional hydrogen-bonded chloride-hydrate assembly $\{[(\text{H}_2\text{O})_4\text{Cl}_2]^{2-}\}_n$. *Z. Naturforschung* **2007**, *62*, 491–494.
- (61) Ghosh, A. K.; Ghoshal, D.; Ribas, J.; Mostafa, G.; Chaudhuri, N. R. Hydrogen-bonded assembly of water and chloride in a 3D supramolecular host. *Cryst. Growth Des.* **2006**, *6*, 36–39.
- (62) Bisht, K. K.; Kathalikkattil, A. C.; Suresh, E. Hydrogen-bonded one- and two-dimensional hybrid water-chloride motifs. *Cryst. Growth Des.* **2012**, *12*, 556–561.
- (63) Dey, B.; Choudhury, S. R.; Gamez, P.; Vargiu, A. V.; Robertazzi, A.; Chen, C.-Y.; Lee, H. M.; Jana, A. D.; Mukhopadhyay, S. Water-chloride and water-bromide hydrogen-bonded networks: influence of the nature of the halide ions on the stability of the supramolecular assemblies. *J. Phys. Chem. A* **2009**, *113*, 8626–8634.
- (64) Casas, J. S.; Couce, M. D.; Sánchez, A.; Sordo, J.; Vázquez López, E. M. Hydrogen bonded water–halide $\{[(\text{H}_2\text{O})_4\text{X}_2]^{2-}\}_n$ (X=Cl, Br) tapes as organizing units in crystals containing $[\text{SnMe}_2(\text{MePN}-\text{H})]^{2+}$ cations (MePN = N-methylpyridoxine). *Inorg. Chem. Commun.* **2013**, *30*, 156–158.
- (65) Braban, M.; Haiduc, I.; Noltemeyer, M.; Roesky, H. W.; Schmidt, H.-G. A supramolecular chloride-water tape of six- and five-membered rings as template in the crystal structure of di- μ -2-hydroxy-bis(diethylenetriamine)dication(II) dichloride trihydrate, $\{[\text{Cu}(\text{dien})(\mu\text{-OH})]^{+}\text{Cl}^{-}\}_2 \cdot 3\text{H}_2\text{O}$. *Inorg. Chem. Commun.* **2008**, *11*, 442–445.

(66) Gilli, G.; Gilli, P. *The Nature of the Hydrogen Bond-IUCr Monographs on Crystallography-23*; Oxford University Press: New York, 2009.

(67) Zhao, J.; Yang, D.; Yang, X.-J.; Wu, B.; Zhao, J.; Yang, D.; Yang, X.-J.; Wu, B. Anion coordination chemistry: From recognition to supramolecular assembly. *Coord. Chem. Rev.* **2019**, *378*, 415–444.

(68) Bowman-James, K. Alfred Werner revisited: The coordination chemistry of anions. *Acc. Chem. Res.* **2005**, *38*, 671–678.

(69) Clark, J. H. Strong hydrogen bonding in oxime solvates of tetra-*n*-butylammonium fluoride. *Can. J. Chem.* **1979**, *57*, 1481–1487.

(70) Tarai, A.; Baruah, J. B. Oxime synthons in the salts and cocrystals of quinoline-4-carbaldoxime for non-covalent synthesis. *CrystEngComm* **2016**, *18*, 298–308.

(71) Tarai, A.; Baruah, J. B. A study on fluoride detection and assembly of hydroxyaromatic aldoximes caused by tetrabutylammonium fluoride. *CrystEngComm* **2015**, *17*, 2301–2309.

(72) Phukan, N.; Baruah, J. B. 3-Hydroxynaphthalene-2-carboxylic acid supported grid-like structure of cadmium chloride coordination polymer with 1,3-bis(4-pyridyl)propane. *J. Mol. Struct.* **2014**, *1076*, 614–619.

(73) Tarai, A.; Baruah, J. B. Inclusion of 2,4-dihydroxybenzaldehyde and 2,4-dihydroxybenzaldoxime in cadmium coordination polymer and conversion of guest aldehyde to oxime. *ChemistrySelect* **2017**, *2*, 11482–11486.

(74) Kalita, D.; Baruah, J. B. Selectivity in metal ions mediated C-N bond formation reactions of 8-aminoquinoline derivatives. *J. Phys. Org. Chem.* **2012**, *25*, 169–175.

(75) Bania, K.; Barooah, N.; Baruah, J. B. Structural variations in self-assembled cadmium benzoate complexes. *Polyhedron* **2007**, *26*, 2612–2620.

(76) Baruah, A. M.; Karmakar, A.; Baruah, J. B. Manganese and cadmium benzoate complexes having 8-aminoquinoline ancillary ligand. *Open Inorg. Chem. J.* **2008**, *2*, 62–68.

(77) Gembicky, M.; Moncol, J.; Lebruskova, K.; Martiska, L.; Valigura, D. Copper(II) 3,5-dinitrosalicylate - the unique System for cocrystal formation by gentle changes in preparation procedure. *Acta Chim. Slovaca* **2008**, *1*, 290–300.

(78) Kalyoncu, S.; Heaner, D. P. Z., Jr.; Kurt, Z.; Bethel, C. M.; Ukachukwu, C. U.; Chakravarthy, S.; Spain, J. C.; Lieberman, R. L. Enzymatic hydrolysis by transition-metal-dependent nucleophilic aromatic substitution. *Nat. Chem. Biol.* **2016**, *12*, 1031–1036.

(79) Lieberman, P.; Somanathan, R. Nitroaromatic compounds: Environmental toxicity, carcinogenicity, mutagenicity, therapy and mechanism. *J. Appl. Toxicol.* **2014**, *34*, 810–824.

(80) Germain, M. E.; Knapp, M. J. Discrimination of nitroaromatics and explosives mimics by a fluorescent Zn(salicylaldimine) sensor array. *J. Am. Chem. Soc.* **2008**, *130*, 5422–5423.

(81) Karmakar, M.; Basak, T.; Chattopadhyay, S. Phosphatase-mimicking activity of a unique penta-nuclear zinc(II) complex with a reduced Schiff base ligand: assessment of its ability to sense nitroaromatics. *New J. Chem.* **2019**, *43*, 4432–4443.

(82) Karmakar, M.; Roy, S.; Chattopadhyay, S. A series of trinuclear zinc(II) complexes with reduced Schiff base ligands: turn-off fluorescent chemosensors with high selectivity for nitroaromatics. *New J. Chem.* **2019**, *43*, 10093–10102.

(83) Ji, N.-N.; Shi, Z.-Q.; Hu, H.-L.; Zheng, H.-G. A triphenylamine-functionalized luminescent sensor for efficient *p*-nitroaniline detection. *Dalton Trans.* **2018**, *47*, 7222–7228.

(84) Barooah, N.; Karmakar, A.; Sarma, R. J.; Baruah, J. B. Self-assembly through hydrogen-bonding and C-H $\cdots\pi$ interactions in metal complexes of N-functionalised glycine. *Inorg. Chem. Commun.* **2006**, *9*, 1251–1254.

(85) Karmakar, A.; Baruah, J. B. Synthesis and characterization of zinc-benzoate complexes through combined solid and solution phase reactions. *Polyhedron* **2008**, *27*, 3409–3416.

(86) Agudelo-Morales, C. E.; Silva, O. F.; Galian, R. E.; Pérez-Prieto, J. Nitroanilines as quenchers of pyrene fluorescence. *ChemPhysChem* **2012**, *13*, 4195–4201.